This presentation participates in OSPP

EGU

Outstanding Student & PhD candidate Presentation contest

Integrated geochemical and mineralogical analysis of heavy metal pollution: A scalable model for global environmental challenges

Amir Joukar[1], Samira Abbasi[2], Javad Darvishi Khatooni[3], and Saeid Pourmorad[4]

[1]Azad university, earth, Iran, Islamic Republic of (amirjoukar992@gmail.com)

[2]Department of Geology, Khorramshahr University of Marine Science and Technology, Iran

[3]Geological Survey and Mineral Explorations of Iran (GSI), Tehran, Iran

[4]University of Coimbra, Centre of Studies in Geography and Spatial Planning (CEGOT), FLUC, Coimbra, Portugal

Abstract

Heavy metal pollution is a major challenge for the environment. It affects more than 30% of global freshwater systems and threatens biodiversity and human well-being. This study presents a comprehensive, interdisciplinary framework that integrates advanced geochemical and mineralogical methods to address this urgent problem and provide scalable solutions with global applicability. Focusing on Aligudarz County in Iran's geologically active Zagros Mountains, 110 sediment samples were analyzed using Inductively Coupled Plasma Mass Spectrometry (ICP-MS) and X-ray Diffraction (XRD). Results revealed the pivotal role of fine-grained silts and clays, particularly Illite and montmorillonite with high adsorption capacities, in heavy metal transport. Pollution indices, including the geo-accumulation index and the enrichment factor, indicate moderate to severe pollution by molybdenum, lead, cadmium and copper. Of particular concern are the traces of cadmium and lead, which pose an acute threat to ecosystems and human health and require immediate action. This study presents a novel method for assessing heavy metal exposure by combining state-of-the-art analytical tools with robust statistical approaches. The results not only provide a basis for targeted mitigation strategies, but also serve as a model for shaping global environmental policy and improving international efforts to protect natural and human systems.

1. INTRODUCTION

In recent years, the relationship between environmental quality and the geochemical properties of Earth materials has attracted increasing attention (Komov, 2021). Improved analytical techniques now allow for more accurate assessment of sediment origin, transport history, and environmental contamination (Rollinson, 2021). Quaternary sediments, particularly in arid and semi-arid regions, often accumulate diverse pollutants from both natural and anthropogenic sources (Heidari & Raheb, 2020). Anthropogenic pollutants such as agricultural runoff, petroleum residues, and industrial discharges are major contributors to environmental degradation (Pourmorad et al., 2021). Among these, heavy metals are of special concern due to their persistence, bioaccumulation potential, and ecological risks (Lee & Khim, 2022). These metals can migrate from contaminated soils and sediments to water resources, agricultural products, and even the atmosphere (Sharma et al., 2020). Unlike many studies focusing solely on human-induced contamination, this research also considers the influence of source rock geochemistry and mineralogy on sediment composition (Roser & Korsch, 1996). The geological and tectonic context of the region shaped by complex structural processes provides an essential foundation for this analysis (Alavi, 2007). The study follows a comprehensive approach: initial geological surveys are conducted to determine the characteristics of the area, followed by geochemical analysis of surface sediments to trace element distribution and potential sources (Abbasi et al., 2021). The environmental risk of heavy metals is then evaluated based on their bioavailability (Zhang, 2021). Given that the study area includes densely populated villages and active agricultural zones, it serves as a suitable model for similar environmental and geochemical investigations worldwide. Furthermore, the integrated methodology used in this research offers a replicable framework combining geochemical data with statistical interpretation (Taylor & McLennan, 1985). The study area is located in the western part of Iran within the boundaries of Aligudarz County, with an approximate geographical position of 49 degrees and 42 minutes east longitude and 33 degrees and 24 minutes north latitude (Dehghani et al., 2022).

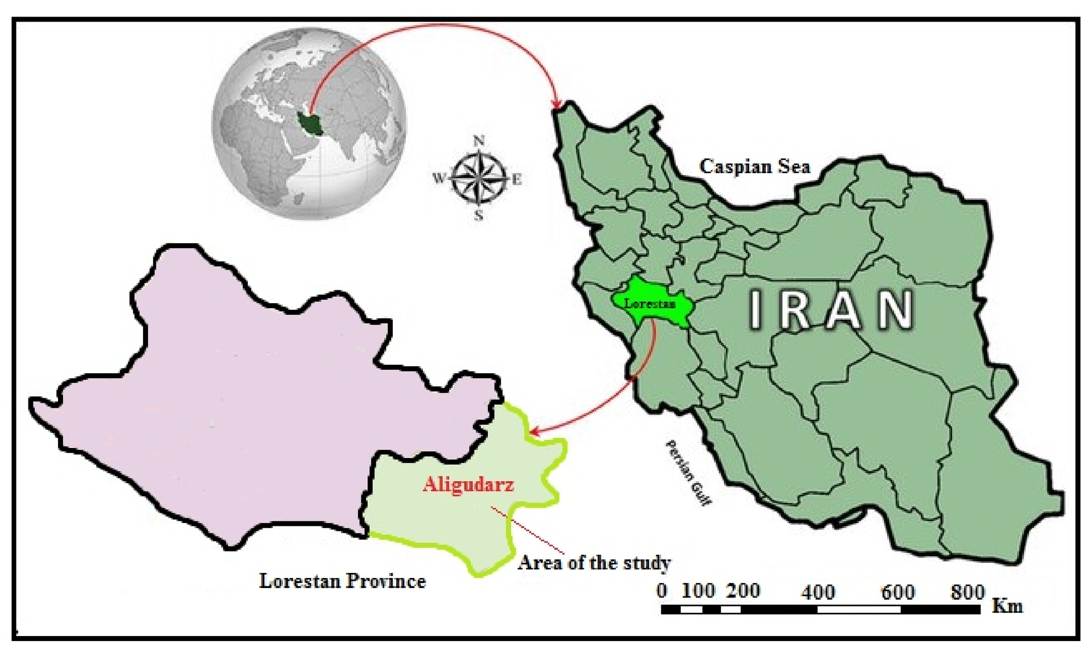

Figure 1:Geographical and geological location of the study area along with the geographical location of the recorded samples (redcircles).

2. Research Methodology:

This study followed a structured and internationally applicable methodology. Initial office-based investigations spanned four months and involved reviewing books, scientific articles, maps, and aerial imagery of the Aligudarz County in southwestern Iran. Subsequently, a three-month fieldwork phase enabled the assessment of sedimentological, tectonic, and mineralogical features, which were crucial in identifying sediment transport paths and optimal sampling sites. A total of 38 surface sediment samples were collected across the study area from mountainous regions to lowlands at a depth of 20 cm to avoid surface contamination. Samples were manually extracted using a hand auger and prepared for laboratory analysis. Geochemical analyses were carried out using ICP-Mass and XRF techniques at the Geological Survey of Iran. The results were statistically processed using SPSS software, involving data distribution assessment, correlation analysis, and element source identification through cluster and factor analysis.

3. Results and discussion

The studies conducted in this research yielded several important findings, summarized as follows, incorporating all referenced tables, figures, and citations:

3.1 Grain Size Analysis:

Particle size analysis of 110 representative samples revealed that the majority of sediments consist predominantly of silt and clay, with an average of 61.59%, followed by sand (25.7%) and gravel (13.56%). The abundance of fine particles like silt and clay plays a key role in pollutant transport from upstream to downstream environments (Morales et al., 2019; Hernandez-Corder, 2019).

3.2 Mineralogical Studies:

Mineralogical analysis (Table 1) identified epidote, quartz, orthoclase, and albite as the dominant minerals, with orthoclase and albite being crucial crustal components contributing to environmental buffering, particularly in mining areas (Zhang et al., 2021; Patel et al., 2021). The samples also contain significant clay minerals such as illite, kaolinite, muscovite, montmorillonite, and chlorite (Van der Meer, 2018), known for their ability to adsorb toxic elements through cation exchange and surface adsorption (MalAmiri et al., 2022). The detection of gypsum indicates possible environmental acidification, while calcite, the only carbonate mineral identified, plays a major role in pH regulation and environmental buffering (Figures 2).

3.3. Elemental Studies:

Geochemical analyses using ICP-MS (Table 2) measured both major and trace elements like Ni, Th, La, V, Y, Co, Ta, Ce, Nb, Ti, Zr, Sc, and Cs, known for retaining geochemical signatures through various environmental processes (Pourmorad et al., 2021; Wang et al., 2022; Ahamad et al., 2021). Figures 3 show that Cu, Zn, and Mn have the highest concentrations, while toxic elements like As and Cd are below 1%, and Pb is around 6%. Despite low concentrations, toxic elements like As, Cd, and Pb pose serious risks to health, including gastrointestinal, neurological, reproductive, and carcinogenic effects (Armstrong-Altrin et al., 2020; Tapia-Fernandez et al., 2017; Sheikh et al., 2020; Bastia et al., 2019; Yongming et al., 2006; Verma et al., 2021).

3.4 Statistical Analysis:

Correlation analysis (Table 3) identified three main clusters of elements, indicating potential common sources: (1) Pb, Mo, As; (2) Pb, Cd, Zn; and (3) Ni, Co. These correlations help trace pollution sources but may be influenced by environmental processes such as oxidation and adsorption (Espejel et al., 2022; Gun and Park, 2020).

3.5 Environmental Index Assessment:

Using global environmental indices Geoaccumulation Index (Igeo), Contamination Factor (Cf), Nemerow Integrated Pollution Index (NIP), and Enrichment Factor (EF) results (Table 4) indicate moderate to severe pollution by Mo, Cu, Pb, and Cd (Izah, 2017). Low to moderate contamination was observed for Mn (2.6%), Ti (1.6%), Ni (2.9%), Nb (1.8%), Pr (1.7%), Gd (1.6%), and Er (3.2%). These indices consistently highlight significant contamination by Mo, Pb, Cd, and Cu, suggesting an urgent need for further investigation and pollution source mitigation (Pourmorad et al., 2022).

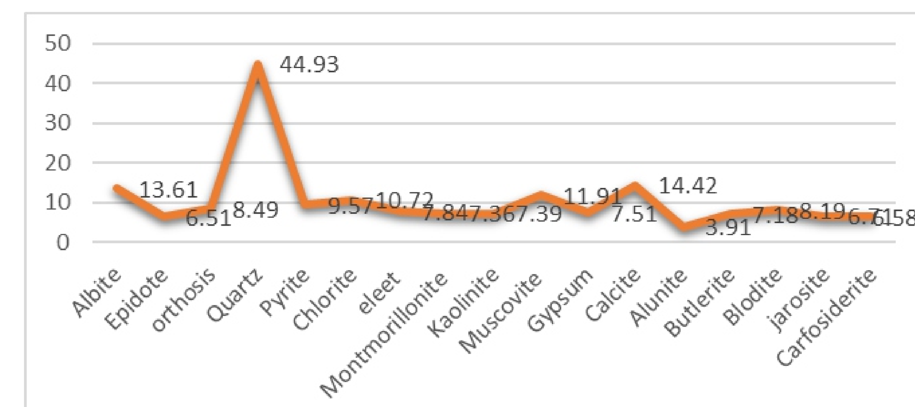

Figure 2 Comparative pie chart of the average percentages of different minerals in the studied samples

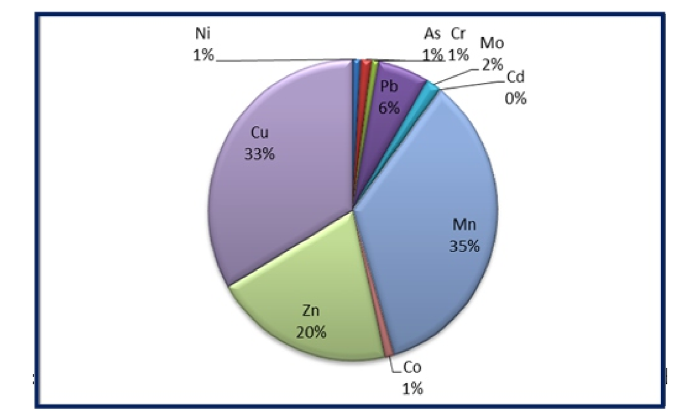

Figure 3: Comparative pie chart of the average percentages of toxic elements in the 110 studied samples (%)

Elements	Minimum	Maximum	Average	Standard Deviation	Range
Albite	3.9	50.1	13.61	10.18	46
Epidote	2.1	10.2	6.51	2.29	8
Orthosis	4.9	11.8	8.49	1.06	7
Quartz	29	72.9	44.93	8.47	46
Pyrite	4.8	22.8	9.57	4.36	19
Chlorite	2.8	28.8	10.72	5.79	25
Eleet	2.1	12.9	7.84	2.19	11
Montmorillonite	2.8	17.8	7.36	3.81	15
Kaolinite	3.9	12.9	7.39	1.81	12
Muscovite	5.2	25.9	11.91	2.96	22
Gypsum	3.1	10.9	7.51	1.71	7
Calcite	1.1	28.8	14.42	8.71	29
Alunite	2.8	6.8	3.91	2.41	4
Butlerite	1.2	13.8	7.18	2.06	14
Blodite	5.1	8.9	8.19	0.49	4
Jarosite	1.9	9.2	6.71	1.89	7
Carfosiderite	3.9	5.9	6.58	0.79	3

Table 1. The results of the statistical study of toxic elements in the studied samples in terms of PPM

Average in the earth's crust	Variation range	Coefficient of variation	Elongation	Bending	Standard Deviation	Average	Maximum	Minimum	Detection value	Element
102	136	0.79	2.36	1.5	27.96	35.92	136	3	1.9	Cr
14	1552.04	1.21	6.39	1.37	303.02	256.17	1571	10.39	1.8	Pb
1.2	311.96	0.94	1.07	1.23	68.96	75.05	318	1.6	2.1	Mo
0.15	21.92	1.71	17.59	3.89	3.61	2.18	22.1	0.07	0.04	Cd
950	6459	0.93	1.37	1.36	1419.39	1561.84	6498	59	0.1	Mn
25	139	0.48	3.71	1.29	20.98	46.02	151	8	0.18	Co
70	3598	0.97	0.87	1.29	856.12	898.16	3672	64	0.2	Zn
60	4782	0.57	4.19	1.53	818.06	1491.24	5102	327	0.2	Cu
84	152	0.67	5.16	1.96	26.14	40.08	159	11	2	Ni
1.8	197.11	0.89	1.38	1.56	47.46	52.01	203	4.5	0.49	As

Table 2. The results of the study of the minerals present in the studied samples (%)

Element	Igeo		EF		Cf		NIPI	
	Pollution class	Percent	class	Percent	Degree of pollution	Percent	Amount	Pollution level
Al	Completely uncontaminated	100	Very low enrichment	100	Low	100	0.45	Completely clean
Mg	Completely uncontaminated	98.7	Very low enrichment	100	Low	91.7	1.39	Little clean
	Uncontaminated to moderate	1.3			Medium	8.3		
Ti	Completely uncontaminated	100	Very low enrichment	98.4	Low	100	0.68	Completely clean
			Medium Enrichment	1.6				
P	Completely uncontaminated	100	Very low enrichment	98.3	Low	100	0.79	Clear
			Medium Enrichment	1.7				
Mn	Completely uncontaminated	100	Very low enrichment	97.4	Low	100	0.69	Completely clean
			Medium Enrichment	2.6				
Mo	Uncontaminated to moderate	78.4	Medium Enrichment	81.6	Low	36	3.07	Polluted
					Medium	53		
	Moderate to severe	21.6	High Enrichment	18.4	High	11		
Zr	Completely uncontaminated	100	Very low enrichment	100	Low	100	0.68	Completely clean
V	Completely uncontaminated	100	Very low enrichment	9٧.7	Low	100	0.73	Clear
			Low to medium Enrichment	2.3				
Cr	Completely uncontaminated	100	No Enrichment	100	Low	100	0.68	Clear
Ni	Completely uncontaminated	97.1	Very low enrichment	98.6	Low	100	0.69	Clear
	Uncontaminated to moderate	2.9	Medium Enrichment	1.4				
La	Completely uncontaminated	100	Very low enrichment	100	Low	100	0.53	Completely clean
Nd	Completely uncontaminated	100	Very low enrichment	100	Low	100	0.52	Completely clean
Cu	Uncontaminated to moderate	83.2	Very low enrichment	77.4	Low	82.4	2.77	Medium
	Moderate to severe	16.8	High Enrichment	13.6	Medium	17.6		
Pb	Uncontaminated to moderate	79.9	Low to medium Enrichment	85.2	Low	76.2	3.1	Polluted
	Moderate to severe	20.1	High Enrichment	14.8	Medium	23.8		

Table 4. The results of the evaluation of environmental indicators (Igeo, EF, Cf, NIPI)

	As	Cd	Co	Cr	Cu	Mo	Ni	Pb	Zn	Fe	Clay
As	1										
Cd	0/48	1									
Co	0/19	-0/02	1								
Cr	0/25	-0/26	0/13	1							
Cu	0/15	0/23	0/17	-0/17	1						
Mo	**0/64**	0/22	-0/03	0/09	0/60	1					
Ni	-0/14	-0/17	**0/74**	**0/68**	0/42	-0/02	1				
Pb	**0/72**	**0/62**	0/12	-0/13	0/19	0/53	0/31	1			
Zn	0/38	**0/74**	0/19	-0/29	0/13	0/22	0/18	**0/79**	1		
Fe	**0/72**	0/28	0/25	0/62	0/32	0/09	0/16	0/43	0/50	1	
Clay	**0/57**	0/30	0/34	0/67	0/59	-0/25	0/26	-0/55	**- 0/6**	0/58	1

Table 3. The results of the correlation study between the studied elements. Separated numbers indicate significant correlation between data.

4. Conclusion

This study provides a comprehensive overview of the sedimentary environment and the extent of toxic element contamination in the region. The predominance of fine particles like silt and clay highlights the potential for pollutant transport. Mineralogical analysis revealed a diverse range of primary, secondary, and clay minerals, indicating complex environmental conditions and possible sources of contamination. Geochemical and environmental index assessments consistently showed moderate to severe levels of pollution, particularly from elements such as molybdenum, lead, cadmium, and copper. The integration of sediment characteristics, mineral composition, and pollution indices offers valuable insight into the region's environmental health and emphasizes the need for further monitoring and management strategies to prevent the spread of contamination.

5. References

Abbasi S., Pourmorad S., Mohanty A. (2021). J. Human, Earth, Future, 2(3); Ahamad A. et al. (2021). Environ. Res., 202; Alavi M. (2007). Am. J. Sci., 307, 1064–1095; Armstrong-Altrin J.S. (2020). J. Palaeogeogr., 9, 28; Bastia F. et al. (2019). Geol. J., 55, 5294–5307; Espejel-García D. et al. (2022). J. Min. Mater. Charact. Eng., 10(6); Gun No S., Park M.E. (2020). Minerals, 10, 49; Hernandez-Hinojosa V. et al. (2019). Carpath. J. Earth Environ. Sci., 13(1), 161–174; Heidari A., Raheb A. (2020). J. Sci. India, 17, 165–179; Komov L. et al. (2021). CRC Press, 400p; MalAmiri N. et al. (2022). Environ. Sci., 286, 131879; Morales J.A. (2019). Morales Journal, 167–192; Patel C.M. et al. (2021). Mater. Today Proc., 43(1), 497–501; Pourmorad S., Mohanty A. (2022). Springer Verlag, 209p; Pourmorad S. et al. (2021). Lithol. Miner. Res., 56, 89–112; Sheikh L. et al. (2020). Open Geosci., 12, 148–162; Tapia-Fernandez H.J. et al. (2017). J. S. Am. Earth Sci., 76, 346–361; Van der Meer F. (2018). Int. J. Appl. Earth Obs., 65; Verma F. et al. (2021). Helion, 7(10); Wang W.H. et al. (2022). Sci. Total Environ., 803, 149980; Yongming H. et al. (2006). Sci. Total Environ., 355, 176–186; Zhang Y. (2021). Geochemical Kinetics, Princeton Univ. Press, 664p.